

A Reanalysis of the UVES M Dwarf Planet Search Program*

R.P. BUTLER,¹ H.R.A. JONES,² F. FENG,¹ M. TUOMI,² G. ANGLADA-ESCUDE,³ AND SANDY KEISER¹

¹*Carnegie Institution for Science
Department of Terrestrial Magnetism
5241 Broad Branch Road NW
Washington, DC 20015-1305, USA*

²*Centre for Astrophysics Research
School of Physics, Astronomy and Mathematics
University of Hertfordshire
College Lane, Hatfield AL10 9AB, UK*

³*School of Physics and Astronomy
Queen Mary University of London
327 Mile End Road, E1 4NS, London, UK*

(Received July 1, 2016; Revised September 27, 2016; Accepted July 10, 2019)

Submitted to ApJ

ABSTRACT

The UVES M Dwarf Planet Search program of Zechmeister, Kurster, & Endl (2009) surveyed 40 M dwarfs and 1 M giant from March 2000 through March 2007. Two of the M dwarfs were double lined spectroscopic binaries. The 38 single-lined M dwarfs in this survey are the nearest and brightest M dwarfs. Starting with the reduced 1-D spectra provided by the UVES team, we re-analyzed the UVES velocities of Proxima Cen as part of the "Pale Red Dot" program (Anglada-Escudé et al. 2016). The velocity RMS decreased from 3.6 to 2.3 m s⁻¹. Motivated by this result, we have harvested all of the raw data from the UVES M Dwarf Planet Search from the ESO archives and have written custom packages to generate 1-D spectra from the raw data, and velocities from the 1-D spectra. The median improvement in the velocity RMS from the new analysis is 1.8 m s⁻¹. Six of the 38 M dwarfs from the original study had a velocity RMS < 4 m s⁻¹. In the reanalysis presented here, 22 of these stars have velocity RMS < 4 m s⁻¹. We improve the upper limits on possible planets orbiting these stars by a factor of typically two to three. For many of these M dwarfs, these observations represent the first epoch of high precision velocity measurements.

Keywords: planetary systems — stars: low mass, brown dwarfs — techniques: radial velocities

1. INTRODUCTION

Prior to the discovery of extrasolar planets, both theory (Boss 1995; Lissauer 1995) and popular imagination (Star Wars, Star Trek) envisioned that most planetary systems would resemble the Solar System, with terrestrial planets orbiting in the inner few AU, giant planets orbiting further out, all in concentric circular orbits ($e < 0.1$). It was not known what fraction of stars might host planets, with estimates ranging from near 0 to nearly 100%.

Not surprisingly the first decade of extrasolar planet discoveries was dominated by giant planets. They are much easier to find. The vast majority of the first 200 planets were found from precision velocity surveys (Butler et al. 2006). What was surprising was the diversity of planetary architecture, including hot jupiters (Mayor & Queloz 1996; Butler et al. 1997) and eccentric planets (Marcy & Butler 1996; Cochran et al. 1997).

Corresponding author: R.P. Butler
paul@dtm.ciw.edu

* Based on observations collected at the European Southern Observatory, Paranal Chile, ESO programs 65.L-0428, 66.C-0446, 267.C-5700, 68.C-0415, 69.C-0722, 70.C-0044, 71.C-0498, 072.C-0495, 173.C-0606, 078.C-0829.

Since well before the detection of extrasolar planets, the main driver of the field has been the desire to detect and study terrestrial mass planets, especially those in the habitable zone where liquid water might plausibly exist on the surface of the planet (Kasting et al. 1993).

When the UVES M Dwarf Planet Search program began in March 2000, fewer than 50 exoplanets were known, only one of which was hosted by an M dwarf (Marcy et al. 1998; Delfosse et al. 1998). All of the known planets at that time were of order a saturn-mass or larger. Compared to solar-type stars, terrestrial mass and potentially habitable planets around M dwarfs are much easier to detect. The lower mass of the host star yields a larger Doppler velocity amplitude. Due to the lower luminosity of M dwarfs, the potentially habitable zone is much closer to the host star. This further increases the Doppler velocity amplitude, and allows many orbits to be observed in a relatively short period of time. The primary problem with observing M dwarfs is their intrinsic faintness.

The UVES M Dwarf team (Kurster et al. 2003) presciently combined the advantages of the large aperture VLT-UT2 telescope with the spectacular new UVES spectrometer (Dekker, et al. 2000), a cross dispersed echelle capable of achieving a resolution of 130,000, to survey 40 nearby M dwarfs and 1 M giant. The M dwarfs were selected to have a $V_{\text{mag}} \leq 12.2$ and a distance within 37 pc (Zechmeister, Kurster, & Endl 2009, hereafter ZKE2009). Active stars were avoided based on their X-ray luminosity (Hunsch et al. 1999). The goal of this program was to probe the nearest M dwarfs with sufficient precision to detect terrestrial mass and potentially habitable planets. The results of this study, spanning eight years, were published in ZKE2009. While no planets were found in this study, it represents a ground breaking effort, combining a bold vision with state-of-the-art instrumentation.

Anthropocentrically the two most interesting M dwarfs are Proxima Cen and Barnard’s star due to their proximity and history (Van de Kamp 1963; Van de Kamp 1969). These two stars were singled out by the UVES M Dwarf team (Endl & Kurster 2008; Kurster et al. 2003). They were able to rule out planets larger than 2-3 Earth in the habitable zone of these stars.

In 2004 the HARPS precision velocity program began observing Proxima Cen. HARPS has been the state-of-the-art precision velocity instrument since its inception (Rupprecht et al. 2004), routinely approaching or exceeding a precision of 1 m s^{-1} (Pepe et al. 2011). The HARPS spectrometer products, including the raw data, reduced spectra, and velocity measurements are available on the ESO archive after a typical embargo period of 1 year ¹.

Traditionally the stabilized spectrometer technique (Eloide, CORALIE, HARPS) has used a binary mask as the template against which Doppler shift measurements are made (Queloz 1995; Pepe et al. 2002). The binary mask differs from zero at the positions of the stellar absorption lines. This is also known as the cross-correlation function method (CCF). In contrast the HARPS-TERRA method (Anglada-Escudé & Butler 2012) uses a “super” stellar template constructed by co-adding all the stellar spectra together. This method makes full use of the information in the stellar spectrum. HARPS-TERRA velocities are constructed directly from the reduced HARPS spectra obtained from the ESO archive.

Highlighting their importance, both Proxima Cen and Barnard’s star were included among the 8 stars examined in the initial HARPS-TERRA paper. The velocity RMS of Proxima Cen from the traditional CCF technique was 2.38 m s^{-1} , while the HARPS-TERRA method yielded an RMS of 2.02 m s^{-1} (Anglada-Escudé & Butler 2012). Subsequent follow up of the HARPS velocity measurements of Proxima Cen taken between 2004 and 2014 as analyzed by the HARPS-TERRA technique revealed possible periodicities in the region of 10 to 20 days, in the potentially habitable zone. This motivated the “Pale Red Dot” program to observe Proxima nearly every night from 19 January to 31 March 2016 (Anglada-Escudé et al. 2016). These high cadence observations quickly revealed a strong periodicity at 11.2 days. A Keplerian fit to the velocities supported the existence of a 1.3 earth-mass planet in the habitable zone. The Doppler semi-amplitude of this signal was 1.4 m s^{-1} .

The UVES M Dwarf team had observed Proxima on 76 nights over 7 years. The velocity RMS of this data set from ZKE2009 was 3.6 m s^{-1} . Starting with the reduced 1D spectra provided by UVES team, we reanalyzed this data with an updated version of our velocity package described in Butler et al. 1996. This yielded an improved velocity RMS of 2.30 m s^{-1} . The dominant periodicity in newly reanalyzed UVES data was at 11.2 days, and the velocities were in phase with the HARPS data (Anglada-Escudé et al. 2016).

This motivated the “Pale Red Dot” team to commence another high cadence HARPS program, focusing on Barnard’s star (Ribas et al. 2018), and the reanalysis of the entire data set from the UVES M dwarf program. We have subsequently harvested all the raw images from the UVES M dwarf program, and the associated calibration frames.

¹ archive.eso.org

We have reduced the raw images to 1-D spectra with our custom raw reduction package, and generated velocities from our precision velocity package. In this latest iteration, the velocity RMS of Proxima Cen has been reduced to 2.02 m s^{-1} . Of the 34 stars in the UVES M dwarf survey with a velocity RMS $< 10 \text{ m s}^{-1}$, the new reduction has decreased the velocity RMS in 33 cases, with a median improvement of 1.8 m s^{-1} .

This paper presents the newly re-analyzed velocities from the UVES M dwarf program. The stars in the UVES M dwarf program are among the nearest and most interesting. This data set achieves a precision that is equal or better than any published result for these stars, demonstrating that UVES is among the finest precision velocity spectrometers in existence. Since we can not go back in time, the first epoch observation of any star is critical. The earliest of these observations predate HARPS by about 4 years.

Section 2 will describe the UVES spectrometer, the data reduction technique, and the updated velocities. Section 3 will examine the new detection thresholds on planet detectability from this data set and compare the results with ZKE2009. The conclusions will be presented in Section 4.

2. RADIAL VELOCITY OBSERVATIONS

The Ultraviolet and Visible Spectrometer (UVES) is a dual-arm cross dispersed echelle spectrometer. UVES is not thermally stabilized. At an elevation of 2,635 m it is not subject to extreme temperature variations². For precision velocity measurements, an Iodine absorption cell is mounted directly in front of the spectrometer entrance (Marcy & Butler 1992), superimposing a dense forest of Iodine lines from 5000 to 6200 angstroms, which serve as a wavelength standard. In addition the shapes of the Iodine lines convey the point-spread-function (PSF) of the spectrometer (Valenti et al. 1995).

The blue arm of the UVES spectrometer covers the Iodine region. For precision velocity measurements either the 0.3" slit (Butler et al. 2004; Kjeldsen et al. 2005), or the fiber slicer (image slicer #3) yielding an effective 0.3" slit (ZKE2009) is used. The resolution of UVES in either mode is 130K, higher than most of the existing precision velocity spectrometers. Figure 1 shows the instrumental point-spread-function (PSF) of UVES compared to other Iodine based instruments. Upon its inception, the Keck/HIRES spectrometer was the state-of-the-art echelle (Vogt et al. 1994). UVES and PFS (Crane et al. 2010) are evidence of the progress in the evolution of echelle spectrometer design over the past generation.

The UVES M dwarf group used the "AUSTRAL" code to model the observed spectra and produce Doppler velocity measurements (Endl, Kurster & Els 2000). The AUSTRAL code is based on the the modeling process outlined in Butler et al. 1996. The UVES M Dwarf survey collected data from March 2000 through March 2007. In 2009 the full UVES data set was published in ZKE2009. Of the 41 stars, two were determined to be double lines spectroscopic binaries (SB2) after two observations. These stars, GJ 190 and GJ 263, were subsequently dropped from the program. Table 1 lists the 39 remaining stars. The first column lists the star name, the second column lists the name assigned by ZKE2009. The spectral type is shown in the third column. The V magnitude is listed in the 4th column. The fifth column is the number of observations. The 6th column lists the velocity RMS from ZKE2009. The 7th column lists the velocity RMS from our analysis. The quadrature difference of the previous two columns is listed in the 8th column.

The spectral type and V magntiude are from Table 2 of ZKE2009, and references therein. The number of observations and the UVES velocity RMS is from Table 4 of ZKE2009. There are five stars that have velocity RMS $> 20 \text{ m s}^{-1}$. These are truly variable. Kurster et al. (2008) have shown that HIP10812 (GJ1046) has a companion with a period of 168.8 d, a semiamplitude of 1830 m s^{-1} , and an eccentricity of 0.278, with an RMS of 3.56 m s^{-1} to the Keplerian fit. We confirm this result, as shown in Figure 2. The minimum (msini) mass of the companion is $27 M_{\text{JUP}}$. As Kurster et al (2008) note, this companion is interesting because of the paucity of brown dwarf companions to solar-like stars and M dwarfs. The RMS of the Keplerian fit to the data in our analysis is 1.77 m s^{-1} , consistent with the improvement in velocity RMS seen in most of the program stars. The four remaining variable stars (HIP 1276, HIP 94997, HIP 61495, HIP 77349) do not have sufficiet observations or temporal coverage for orbital determination.

Of the remaining 34 stars, for only one case did the newly reduced velocities have a velocity RMS larger than that reported by ZKE2009. The UVES velocity RMS for HIP 17766 (HG7-15) is 8.7 m s^{-1} . Our RMS is 8.91 m s^{-1} . This star has the largest velocity RMS of any of the 34 "stable" stars. This is also the only star with measurement uncertainty larger than the velocity scatter in ZKE2009. This star was quickly dropped from the UVES program.

² (<https://www.eso.org/sci/facilities/paranal/astroclimate/site.html#CliInfo>)

Table 1. UVES M Dwarf Planet Search

Star	ZKE2009	Spectral	V (mag)	N_obs	U_RMS	V_RMS	Quadrature
	name	type					Difference
HIP56466	GJ3671	M0	11.20	12	5.6	3.65	4.25
HIP82283	GJ3973	M1.5Vk:	10.94	5	6.8	3.72	5.69
HIP63550	GJ3759	M1V	10.95	11	3.9	3.08	2.39
GL433	GJ433	M1.5	9.79	54	4.4	3.55	2.60
HIP55042	GJ422	M3.5	11.66	15	4.0	3.77	1.34
HIP104059	GJ817	M1	11.48	25	4.9	2.71	4.08
GL551	Proxima	M5.5Ve	11.05	76	3.6	2.02	2.98
GL699	Barnard	M4Ve	9.54	75	3.3	2.58	2.06
HIP86214	GJ682	M3.5	10.96	20	4.0	3.33	2.22
HIP93206	GJ739	M2	11.14	19	4.4	3.59	2.54
HIP110534	GJ855	M0.5	10.74	22	5.8	5.26	2.44
HIP104432	GJ821	M1	10.87	35	5.0	1.63	4.73
HIP22762	GJ180	M2	12.50	24	3.8	3.11	2.18
HIP80268	GJ620	M0	10.25	5	7.3	4.19	5.98
HD225213	GJ1	M1.5	8.57	24	2.5	2.05	1.43
HD42581	GJ229	M1/M2V	8.14	32	5.5	4.79	2.70
HIP114411	GJ891	M2V	12.20	25	7.5	3.77	6.48
HIP47103	GJ357	M2.5V	10.85	30	5.3	3.35	4.11
HIP13389	GJ118	M2.5	10.70	26	6.5	5.70	3.12
HIP19165	GJ160.2	M0V	9.69	33	8.1	5.44	6.00
HIP21556	GJ173	M1.5	10.35	12	5.3	3.02	4.36
HIP27359	GJ218	M1.5	10.72	9	3.1	2.23	2.15
HIP49091	GJ377	M3	11.44	14	6.7	2.91	6.04
HIP65520	GJ510	M1	11.05	23	5.6	4.02	3.90
HIP82256	GJ637	M0.5	11.36	17	6.4	3.56	5.32
HIP108569	GJ842	M0.5	9.74	17	6.7	2.92	6.03
HIP117886	GJ911	M0V	10.88	17	14.9	3.24	14.5
HIP7170	GJ3098	M1.5Vk:	11.21	9	9.1	5.37	7.35
HIP5812	GJ3082	M0	11.10	10	6.2	5.08	3.55
HIP1734	GJ1009	M1.5	11.16	22	5.3	4.53	2.75
HIP112452	GJ4293	M0.5	10.90	14	8.7	4.78	7.27
HIP3143	GJ27.1	M0.5	11.42	30	6.1	4.27	4.36
HIP37978	GJ1100	M0	11.48	12	9.3	3.78	8.50
HIP17766	HG7-15	M1V	10.85	11	8.7	8.91	
HIP1276	GJ3020	M2.5	11.54	13	298.8	330.0	
HIP94997	GJ4106	M2	10.82	5	20.7	28.6	
HIP61495	GJ477	M1	11.08	8	3486.0	3487.7	
HIP77349	GJ3916	M2.5V	11.25	6	2107.7	2211.0	
HIP10812 ^a	GJ1046	M2.5+v	11.62	14	1248	1245	

^aKeplerian fit: p=168.8d, K=1828, e=0.28, Msini=32 Mjup, RMS=1.77 m/s

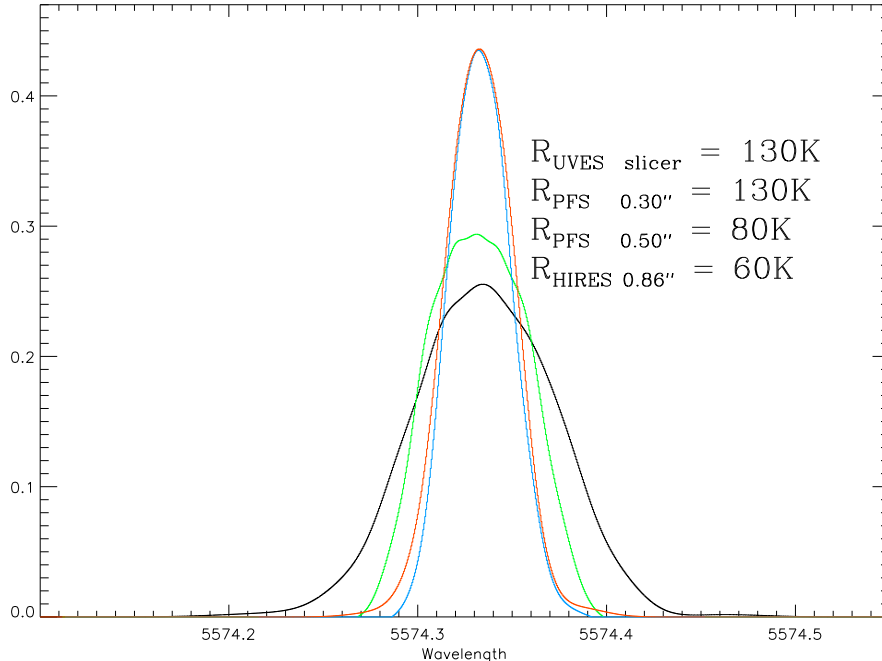


Figure 1. The point-spread-function (PSF) of echelle spectrometers with an Iodine cell, in the middle of the Iodine absorption region. In each case the PSF is from an observation of a star, taken through the Iodine absorption cell. The red PSF is from UVES, taken through the fiber-slicer, which yields an effective slit width of 0.3". Blue and green are from PFS with slit widths of 0.3" and 0.5" respectively. HIRES is shown in black. The slit width and resolution of each spectrometer is listed in the figure.

For the 33 stars that have a velocity RMS $< 6 \text{ m s}^{-1}$, our RMS is significantly reduced compared to ZKE2009. If we assume that sources for velocity scatter add in quadrature, then the final velocity RMS for any given star is given by: $\sqrt{J^2 + P^2 + N^2 + R^2}$. Where J is the contribution from stellar jitter, P is the contribution from orbiting planets, N is the contribution from photon noise, and R is the contribution from the velocity reduction package.

For each star in this program, the same data has now been analyzed by independent raw reduction and velocity reduction packages. For each star the velocity RMS contributions from stellar jitter (J), orbiting planets (P), and photon noise (N) is identical, only the contribution from the reduction packages differ. The reduction in the velocity scatter due to the reduction package (R) can be estimated as the quadrature difference of the velocity RMS of the original UVES data set with respect to the new reduction. This is shown in the final column of Table 1. The median reduction in "R", the velocity scatter due to the Doppler velocity reduction code, is 4 m s^{-1} .

Velocities for the 35 stars with velocity RMS $< 30 \text{ m s}^{-1}$ are shown in Figure 1 of ZKE2009. We have reproduced this with our newly reduced data as shown in Figure 3. To allow direct comparison of the two velocity sets, we have used the same scaling, figure arrangement, and stellar names as shown in ZKE2009.

The most obvious difference between Figure 1 of ZKE2009 and Figure 3 are the stars with significant proper motion, notably Barnard's star (GL 699). The barycentric corrections computed in ZKE2009 do not include proper motion. Each star is assumed to have fixed coordinates. Table 3 of ZKE2009 provides a model of the secular acceleration due to proper motion for the program stars. This correction is shown as a linear fit to the velocities for the high proper motion stars in Figure 1 of ZKE2009. The RMS of the ZKE2009 velocities includes their correction for secular acceleration.

Our barycentric correction code includes the stellar proper motion information. The stellar coordinates are advanced by the proper motion. Our final barycentric correction includes the effect of proper motion, so the resulting velocities do not show the effect of secular acceleration.

The two stars in Figure 3 with the largest velocity scatter (HIP94997/GJ4016 and HIP17766/HG7-15) also have the largest measurement uncertainty. For all of the remaining 33 stars, with velocity RMS $< 6 \text{ m s}^{-1}$, the velocity RMS from our new reduction package is improved. The median velocity RMS improvement is 1.8 m s^{-1} . The median quadrature difference difference in the velocity RMS is 4 m s^{-1} .

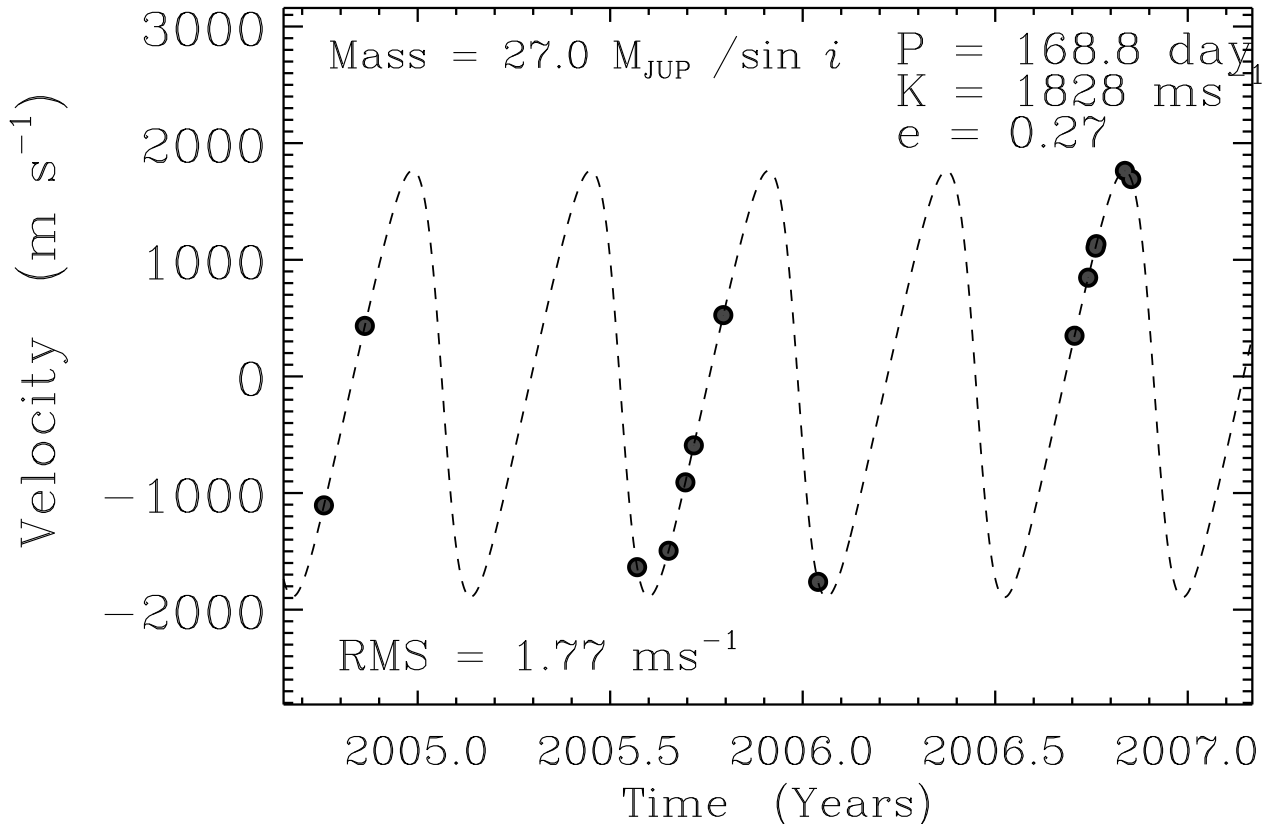


Figure 2. Keplerian fit to the velocities of HIP 10812 (GJ 1046)

The stars in this program were observed one to three times each night. ZKE2009 averaged all observations taken in a single night. We have followed this protocol in comparing the results of this study (Table 1 and Figure 3). The electronic table of velocities in this paper provides the results for every observation. An example of this table is given in the Appendix.

3. DETECTION LIMITS

The UVES team estimated detection limits by injecting signals into their data, then attempting to recover them with periodograms, as shown in Figure 6 of ZKE2009. This approach can be sensitive to injected signals and avoids sampling the period range where significant periodogram powers are found.

We find and constrain signals using the adaptive Markov Chain Monte Carlo (MCMC) algorithm called “DRAM” introduced by Haario et al. (2006) and applied in Tuomi et al. (2014) and Feng et al. (2017). To explore the parameter space efficiently, we run multiple tempered (hot) chains to find local posteriori maxima and constrain these maxima using untempered (cold) chains. The algorithm is stopped when the inclusion of a new signal into the model does not increase the likelihood such that the Bayes factor is larger than 150 (Kass & Raftery 1995; Feng et al. 2016). We adopt the noise model comparison scheme introduced by Feng et al. (2017) to choose the optimal order of moving average (MA) models. We adopt a semi-Gaussian prior ($P(e) = \mathcal{N}(0, 0.2)$ and $e > 0$, Feng et al. 2016) for eccentricity and uniform priors for logarithmic period and other Keplerian parameters.

Following Tuomi et al. (2014), we determine the detection limit using the posterior samples drawn by multiple MCMC chains. For a data set with N signals detected, the MCMC chains for the $N + 1$ -signal model would only explore the parameter space where additional signals could exist. Thus the boundary of unexplored parameter space for the $N + 1$ signal defines the detection limit for a given data set. Since the posterior distribution is probabilistic, the detection limit should also be probabilistic. Thus we show probabilistic detection limits in Figure 4 to compare with the detection limits shown in figure 6 of ZKE2009.

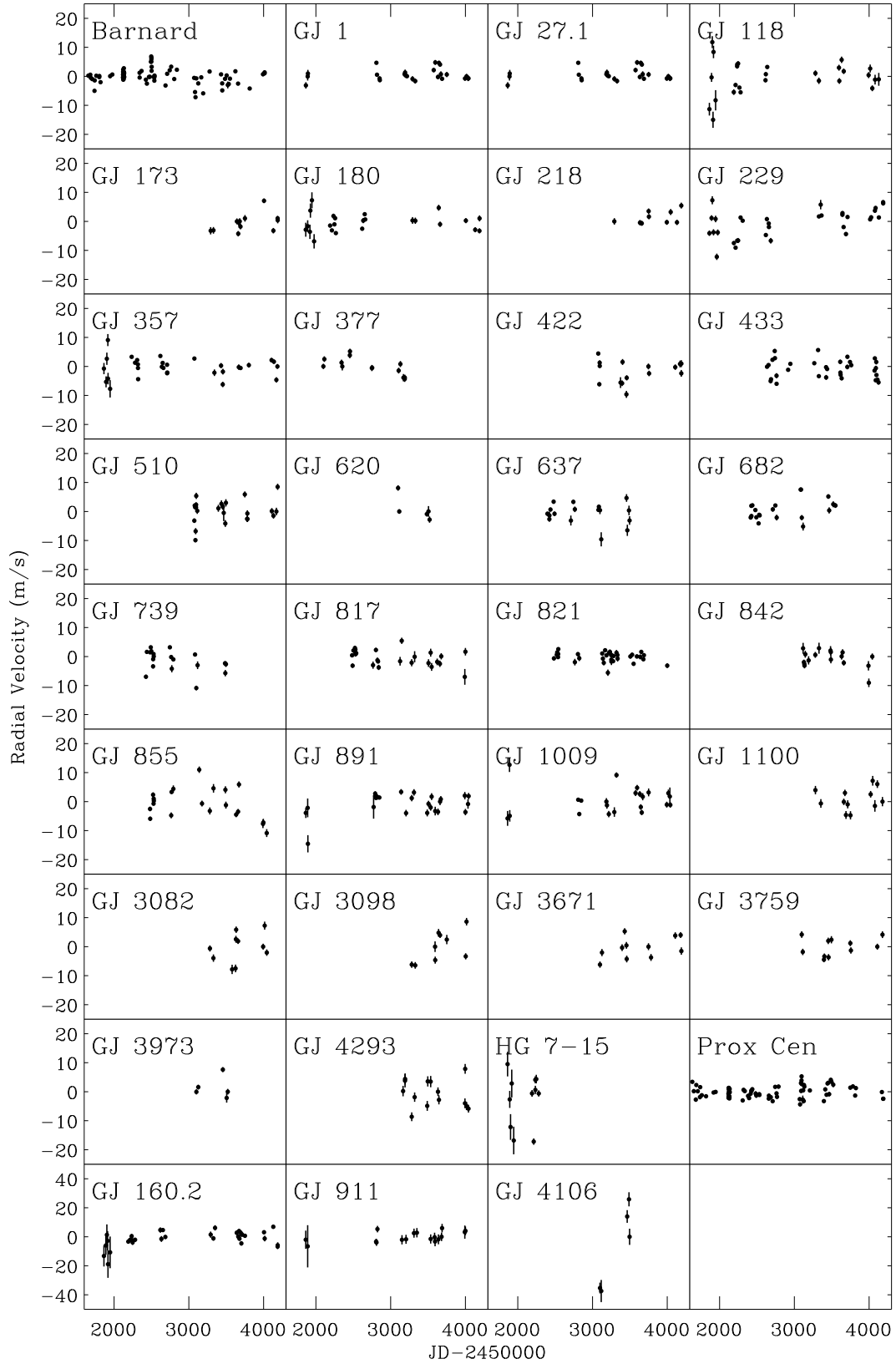


Figure 3. Radial Velocities for 35 M dwarfs from the UVES M dwarf planet survey.

Given the improved velocity precision of our data set, it is not surprising that the detection limit is about 2 or 3 times lower than in ZKE2009 for the habitable zone of Barnard’s star. This also applies to other stars and does not depend on whether signals are identified or not. The upper limits of planetary mass for the habitable zones of Barnard’s star, GJ 180, GJ 357, GJ 433, GJ 682, GJ 817, GJ 821, GJ 891, and Proxima Centauri are less than $10 M_{\oplus}$. Hence our new reduction of UVES data has significantly improved detection limits compared with that of ZKE2009 and demonstrates that these data sets are capable of detecting temperate Earth-like planets around M dwarfs.

A number of the identified signals maybe consistent with Earth-sized planets. The periods of the signals for GJ 118 is 1.06 d, for GJ 160.2 17.34 d, for GJ 357 3.93 d, for GJ422 20.26 d, for GJ 433 7.37 and 71.99 d, for GJ 682 1.42 d, for GJ739 3.70 d, for GJ 855 68.63 d, for GJ 1009 2.11 d, and for HG 7-15 1.19 d. Some of these signals are reported in the literature such as GJ 433 b with a period of 7.37 d (Tuomi et al. 2014). Some of these signals differ from the signals reported in the literature due to a lack of combined analysis with other RV data sets. For example, GJ 422 b has an orbital period of about 26.16 ± 0.04 d (Tuomi et al. 2014) while a signal around 20.26 d is found in the new UVES data. A combined analyses of these UVES data with other data extending the baseline and increasing the number of epochs will be necessary to quantify these signals.

4. CONCLUSION

When the UVES M Dwarf Planet search begin in 2000, the least massive known exoplanet planet was 30% larger than Saturn. There were only a handful of teams that had developed precision velocity capabilities. State-of-the-art precision ranged from 3 to 10 m s^{-1} . The decision by the UVES M Dwarf Planet team to chase potentially habitable planets with an untested instrument was courageous. They would need to push velocity precision to the 1 m s^{-1} level.

Data reduction packages are not usually considered as a source of measurement uncertainty. A Doppler velocity shift of 1 m s^{-1} on an extraordinary spectrometer like UVES is slightly less than one-thousandth of a pixel on the CCD, or about 7 Silicon atoms on the CCD substrate. Achieving and maintaining this level of precision is difficult. On UVES this is further complicated because it is a general purpose echelle spectrograph, used by programs with widely different wavelength coverage and resolution requirements. Major elements including the gratings and slit move. An optional fiber slicer can be used in place of the slit.

UVES differs from purpose built precision velocity echelles, such as HARPS and PFS, where stability is valued above everything. The first rule of a purpose built precision velocity echelle is that nothing moves, with the possible exception of the focus. This makes the results from UVES all the more remarkable. Beginning in March 2000 UVES spectra have recorded spectra with sufficient information content to approach 1 m s^{-1} precision. This data set has now been reduced to 1D spectra with independently written raw reduction packages, and analyzed with independently written Doppler velocity packages. All of the sources of velocity RMS (photon-noise, stellar jitter, unknown planets) are identical, the only source of difference are the data analysis packages themselves. Our Doppler velocity package is a direct descendent of Butler et. al. (1996). This package is also producing 1 m s^{-1} precision with PFS data. We are preparing a manuscript “On Achieving 1 m s^{-1} Doppler Precision with an Iodine Absorption Cell”.

The most important observation in a precision velocity data set is the first because observers can not go back in time. For most of the stars in the UVES M Dwarf program, these are the first observations taken with state-of-the-art precision. This data set is all the more remarkable for focusing on the nearest stars, and the stars most likely to harbor detectable potentially habitable planets. These observations will continue to be important in finding and constraining planets around these stars for decades to come. We do not expect this to be the final word on this remarkable data set. We look forward to future researchers re-analyzing this data set with a superior Doppler reduction package, and producing the surprises that emerge from better measurement precision.

This paper is dedicated to Sandy Keiser. Sandy passed away suddenly during the analysis of this data set. Sandy was a DTM astronomer and system manager who collaborated with many of the DTM astronomers. Her work was critical to this paper, and many of the precision velocity papers we have produced. We are grateful to the UVES M Dwarf team for having the courage and foresight to take on this extraordinary program. Starting back in the infancy of precision velocity measurements, they boldly went straight to the heart of the most interesting and challenging problem, finding potentially habitable planets around the nearest stars. This research has made use of the services of the ESO Science

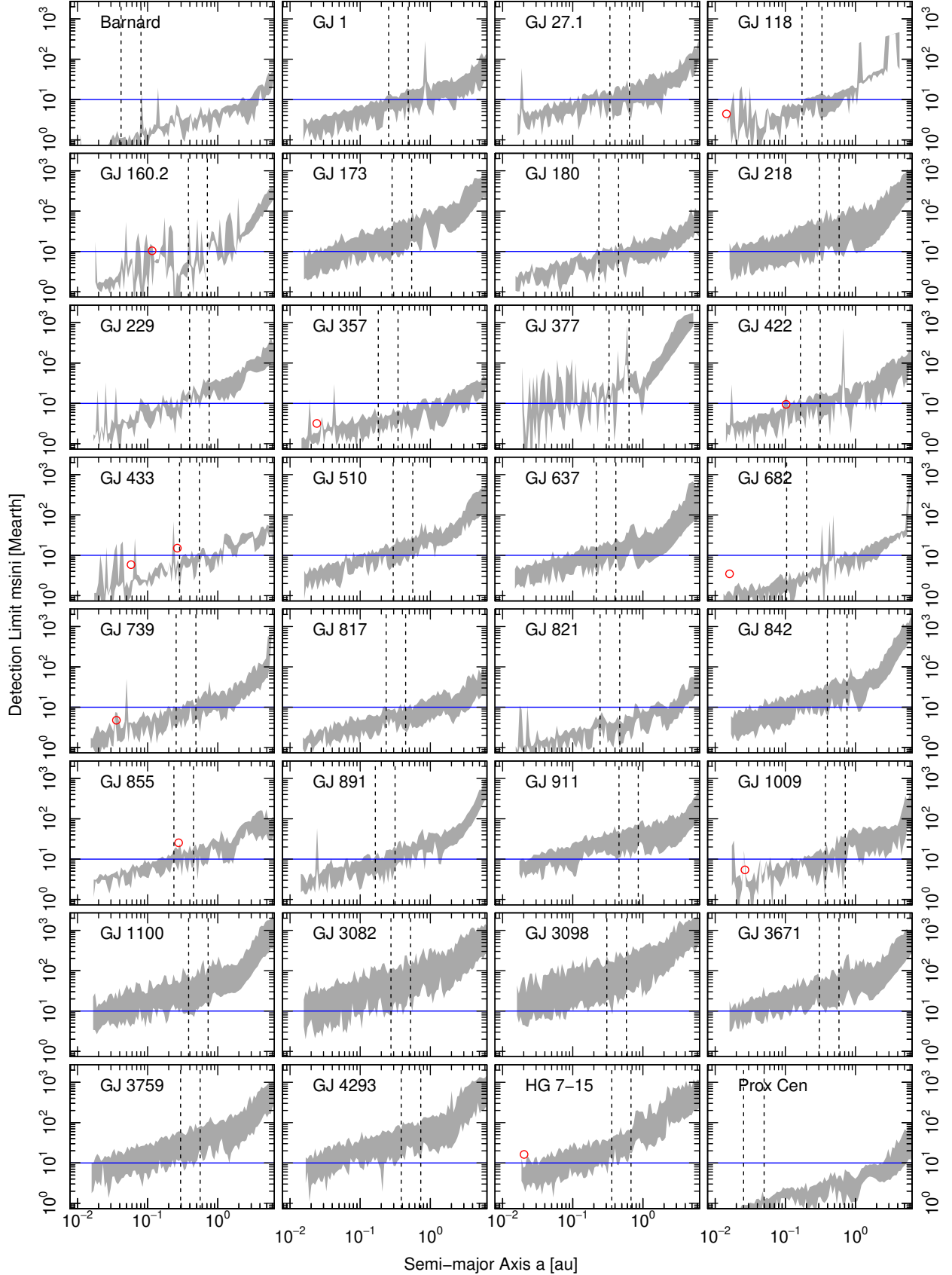


Figure 4. Probabilistic detection limits for the new UVES data of 34 M dwarfs. The N statistically significant signals found in a given data set are denoted by red circles. The grey region in each panel shows the probabilistic detection limit which is defined by the 50% quantile of the posterior distribution of semi-amplitude ($K_{50\%}$) and the maximum of semi-amplitude K_{\max} in the posterior samples for the $N + 1$ signal. The habitable zone denoted by dashed lines is calculated using method introduced by Kopparapu et al. (2014). The blue horizontal line represents the $10 M_{\oplus}$ limit.

Archive Facility, NASA's Astrophysics Data System Bibliographic Service, and the SIMBAD database, operated at CDS, Strasbourg, France,

APPENDIX

A. APPENDIX INFORMATION

Table 3. New reduction of UVES data for 35 M dwarfs.

Star	BJD (day)	RV (m/s)	RV error (m/s)
GL699	2451655.72529	1.79	1.13
GL699	2451655.72921	0.05	1.22
GL699	2451655.73309	-1.26	1.17
GL699	2451681.80795	0.89	1.06
GL699	2451681.81196	-0.73	0.98
GL699	2451681.81573	2.28	1.29
GL699	2451688.66317	-1.28	0.91
GL699	2451688.66714	-0.42	0.9
GL699	2451688.67106	0.14	0.88
GL699	2451707.67233	-1.03	0.88

NOTE—Table 3 is published in its entirety in the machine-readable format. A portion is shown here for guidance regarding its form and content.

REFERENCES

- Anglada-Escudé, G. & Butler, R.P. 2012, *ApJS*, 200, 15
- Anglada-Escudé, G., Amado, P.J., Barnes, J., Berdiñas, Zaira M., Butler, R.P., Coleman, G.A.L., de La Cueva, I., Dreizler, S., Endl, M., Giesers, B., Jeffers, S.V., Jenkins, J.S., Jones, H.R.A., Kiraga, M., Kürster, M., López-González, M.J., Marvin, C.J., Morales, N., Morin, J., Nelson, R.P., Ortiz, J.L., Ofir, A., Paardekooper, S., Reiners, A., Rodríguez, E., Rodríguez-López, C., Sarmiento, L.F., Strachan, J.P., Tsapras, Y., Tuomi, M., & Zechmeister, M 2016, *Nature*, 536, 437
- Boss, A.P. 1995, *Science*, 267, 360
- Butler, R.P., Marcy, G.W., Williams, E., McCarthy, C. & Vogt, S.S. 1996, *PASP*, 108, 500
- Butler, R.P., Marcy, G.W., Williams, E., Hauser, H. & Shirts, P. 1997, *ApJ*, 474, L115
- Butler, R.P., Bedding, T.R., Kjeldsen, H., McCarthy, C., O'Toole, S.J., Tinney, C.G., Marcy, G.W. & Wright, J.T. 2004, *ApJ*, 600, L75
- Butler, R.P., Wright, J.T., Marcy, G.W., Fischer, D.A., Vogt, S.S., Tinney, C.G., Jones, H.R.A., Carter, B.D., Johnson, J.A., McCarthy, C. & Penny, A.J. 2006, *ApJ* 646, 505
- Cochran, W.D., Hatzes, A.P., Butler, R.P. & Marcy, G.W. 1997, *ApJ*, 483, 457
- Crane, J.D., Shtetman, S.A., Butler, R.P., Thompson, I.B., Birk, C., Jones, P. & Burley, G.S. 2010, *SPIE*, 7735, 53
- Dekker, H., D'Odorico, S., Kaufer, A., Delabre, B. & Kotzłowski, H. 2002, *SPIE*, 4008, 534
- Delfosse, X., Forveille, T., Mayor, M., Perrier, C., Naef, D. & Queloz, D. 1998, *A&A*, 338, L67
- Endl, M., Kürster, M. & Els, S. 2000, *A&A*, 362, 585
- Endl, M. & Kürster, M. 2008, *A&A*, 488, 1149
- Feng, F., Tuomi, M., & Jones, H. R. A. 2017a, *MNRAS*, 470, 4794
- Feng, F., Tuomi, M., Jones, H. R. A., Butler, R. P., & Vogt, S. 2016, *MNRAS*, 461, 2440

- Haario, H., Laine, M., Mira, A., & Saksman, E. 2006, *Statistics and Computing*, 16, 339
- Hünsch, M., Schmitt, J.H.M.M., Sterzik, M.F. & Voges, W. 1999, *A&A*, 135, 319
- Kasting, J.F., Whitmire, D.P. & Reynolds, R.T. 1993, *Icarus*, 101, 108
- Kass, R. E., & Raftery, A. E. 1995, *Journal of the american statistical association*, 90, 773
- Kjeldsen, H., Bedding, T.R., Butler, R.P., Christensen-Dalsgaard, J., Kiss, L.L., McCarthy, C., Marcy, G.W., Tinney, C.G. & Wright, J.T. 2005, *ApJ*, 635, 1281
- Kopparapu, R. K., Ramirez, R. M., SchottelKotte, J., et al. 2014, *ApJL*, 787, L29
- Kürster, M., Endl, M., Rouesnel, F., Els, S., Kaufer, A., Brilliant, S., Hatzes, A.P., Cochran, W.D. 2003, *Astronomische Nachrichten*, 324, 4
- Kürster, M., Endl, M., Rouesnel, F., Els, S., Kaufer, A., Brilliant, S., Hatzes, A.P., Saar, S.H. & Cochran, W.D. 2003, *A&A*, 403, 1077
- Kürster, M., Endl, M. & Reffert, S. 2008, *A&A*, 483, 869
- Lissauer, J.J. 1995, *Icarus*, 114, 217
- Marcy, G.W. & Butler R.P. 1992, *PASP*, 104, 270
- Marcy, G.W. & Butler R.P. 1996, *ApJL*, 464, L151
- Marcy, G.W., Butler, R.P., Vogt, S.S., Fischer, D.A. & Lissauer, J.J. 1998, *ApJ*, 505, L147
- Mayor, M. & Queloz, D. 1995, *Nature*, 378, 355
- Pepe, F., Mayor, M., Galland, F., Naef, D., Queloz, D., Santos, N.C., Udry, S. & Burnet, M. 2002, */aap*, 388, 632
- Pepe, F., Lovis, C.e Ségransan, D., Benz, W., Bouchy, F., Dumusque, X., Mayor, M., Queloz, D., Santos, N.C., Udry, S. 2011, *A&A*, 534, 58
- ueloz, D. 1995, PhD Thesis 2788, University of Geneva
- Ribas, I. et al. 2018, *Nature*, submitted
- Rupprecht, G., Pepe, F., Mayor, M., Queloz, D., Bouchy, F., Avila, G., Benz, W., Bertaux, J., Bonfils, X., Dall, Th., Delabre, B., Dekker, H., Eckert, W., Fleury, M., Gilliotte, A., Gojak, D., Guzman, J.C., Kohler, D., Lizon, J., Lo Curto, G., Longinotti, A., Lovis, C., Megevand, D., Pasquini, L., Reyes, J., Sivan, J., Sosnowska, D., Soto, R., Udry, S., Van Kesteren, A., Weber, L. & Weilenmann, U. 2004, *SPIE*, 5492, 148
- Tuomi, M., Jones, H. R. A., Barnes, J. R., Anglada-Escudé, G., & Jenkins, J. S. 2014, *MNRAS*, 441, 1545
- Valenti, J.A., Butler, R.P., & Marcy, G.W. 1995, *PASP*, 107, 966
- van de Kamp, P. 1963, *AJ*, 68, 515
- van de Kamp, P. 1969, *AJ*, 74, 757
- Vogt, S.S., Allen, S.L., Bigelow, B.C., Bresee, L., Brown, B., Cantrall, T., Conrad, A., Couture, M., Delaney, C., Epps, H.W., Hilyard, D., Hilyard, D.F., Horn, E., Jern, N., Kanto, D., Keane, M.J., Kibrick, R.I., Lewis, J.W., Osborne, J., Pardeilhan, G.H., Pfister, T., Ricketts, T., Robinson, L.B., Stover, R.J., Tucker, D., Ward, J. & Wei, M. Z. 2004, *SPIE*, 2198, 362
- Zechmeister, M., Kurster, M. & Endl, M. 2009, *A&AS*, 505, 859